

DOI: 10.1002/ pssa.201800856R2

Article type: **Full Paper**

Near-Surface [Ga]/([In]+[Ga]) Composition in Cu(In,Ga)Se₂ Thin-Film Solar Cell Absorbers – An Overlooked Material Feature

Roberto Félix, Wolfram Witte, Dimitrios Hariskos, Stefan Paetel, Michael Powalla, Mickael Lozac'h, Shigenori Ueda, Masatomo Sumiya, Hideki Yoshikawa, Keisuke Kobayashi, Wanli Yang, Regan G. Wilks, and Marcus Bär*

Dr. R. Félix, Dr. R. G. Wilks, Prof. M. Bär
Interface Design
Helmholtz-Zentrum Berlin für Materialien und Energie GmbH
14109 Berlin, Germany
Email: roberto.felix_duarte@helmholtz-berlin.de

Dr. W. Witte, Dr. D. Hariskos, Dr. S. Paetel, Prof. M. Powalla
Zentrum für Sonnenenergie- und Wasserstoff-Forschung Baden-Württemberg (ZSW)
70563 Stuttgart, Germany

Dr. M. Lozac'h, Dr. M. Sumiya
National Institute for Materials Science (NIMS)
Tsukuba 305-0044, Japan

Dr. S. Ueda, Dr. H. Yoshikawa
Synchrotron X-ray Station at SPring-8
National Institute for Materials Science (NIMS)
Hyogo 679-5148, Japan

Dr. S. Ueda
Research Center for Advanced Measurement and Characterization
National Institute for Materials Science (NIMS)
Tsukuba 305-0047, Japan

Prof. K. Kobayashi
Quantum Beam Science Directorate
Japan Atomic Energy Agency
Hyogo 679-5148, Japan

Dr. W. Yang
Advanced Light Source (ALS)
Lawrence Berkeley National Laboratory
Berkeley 94720, USA

Dr. R. G. Wilks, Prof. M. Bär
Energy Materials In-Situ Laboratory (EMIL)
Helmholtz-Zentrum Berlin für Materialien und Energie GmbH
12489 Berlin, Germany

Prof. M. Bär

Helmholtz-Institute Erlangen-Nürnberg for Renewable Energy, Forschungszentrum Jülich, Egerlandstr. 3, 91058 Erlangen, Germany

Prof. M. Bär

Physical Chemistry II, Department of Chemistry and Pharmacy, Friedrich-Alexander-Universität Erlangen-Nürnberg, Egerlandstr. 3, 91058 Erlangen, Germany

Keywords: chalcopyrites, thin-film solar cells, surface band gap, photoemission spectroscopy

The chemical and electronic structure in the near-surface region of Cu(In,Ga)Se₂ thin-film solar cell absorbers is investigated using non-destructive soft and hard x-ray photoelectron spectroscopy. In addition to a pronounced surface Cu-depletion, a [Ga]/([In]+[Ga]) profile indicates that the topmost surface is Ga-poor (or In-rich). For the studied depth region, common depth profiling techniques generally fail to provide reliable information and, thus, the near-surface chemical and electronic structure profile is often overlooked. The relation between the observed near-surface elemental compositions and the derived electronic properties of the absorber material is discussed. It is found that the surface band gap energy crucially depends on the Cu-deficiency of the absorber surface and suggests that it is – in this region – only secondarily determined by the [Ga]/([In]+[Ga]) ratio.

1. Introduction

Thin-film solar cell devices based on chalcopyrites [Cu(In_{1-x}Ga_x)(S_ySe_{1-y})₂, CIGSSe] as the absorber material have exhibited a surge in power conversion efficiencies, η , in the last couple of years.^[1] Many laboratories have, in fact, produced chalcopyrite-based thin-film solar cells with η surpassing the 20%-threshold on the laboratory-scale^[1,2] (record η : 22.9%^[1a]), demonstrating a performance similar to, if not higher than, that of multicrystalline Si-wafer-based solar device technology (record η : 22.3%^[3]). Although a great deal of insight into the working mechanisms of chalcopyrite-based solar cells has been gained throughout the past years, advances in efficiency for this type of device have generally been obtained through

empirical approaches in the synthesis process of the devices; the latest η gains have certainly been related to the addition of (heavy) alkali elements.^[1a,1b,1c]

Another means to optimize solar cell performance has been the so-called band gap (E_g) grading by (aiming for) a deliberate tailoring of the $[\text{Ga}]/([\text{In}]+[\text{Ga}])$ ratio throughout the absorber bulk.^[4] For controlling these optimization efforts, destructive depth profiling techniques have been typically used that are based on etching through the absorber thin-film by way of high energy ion sputtering or plasma treatments.^[1b,1c,1e,5] However, these techniques generally only result in reliable composition data after equilibrium etching conditions are established. Thus, corresponding composition profiles in the near-surface region of samples – at best – always have a significant experimental uncertainty.^[5] This information, however, is crucial as the composition (and, thus, electronic structure) at the sample surface determines the energy level alignment with a potential junction partner.

In this work, we have performed excitation energy-dependent photoemission measurements to non-destructively derive the composition in the near-surface region of industry-relevant $\text{Cu}(\text{In,Ga})\text{Se}_2$ (CIGSe) thin-film solar cells absorbers. We present and discuss related challenges and our findings on surface Cu- and $[\text{Ga}]/([\text{In}]+[\text{Ga}])$ -related composition deviations, and their direct effect on the electronic structure of the absorber near-surface region. In detail, based on the derived surface elemental composition of the absorber, a proposed range of surface band gap (E_g^{surf}) values from literature is compared with the band gap values calculated solely considering the elemental $[\text{Ga}]/([\text{In}]+[\text{Ga}])$ composition of the absorber derived from the different excitation-energy-dependent measurements. The findings of this approach highlight the need for direct means of E_g^{surf} measurement.

2. Results and Discussion

The x-ray photoelectron spectroscopy (XPS) survey spectra of the studied CIGSe absorbers (see Figure S1, Supporting Information) display the photoemission and Auger lines of the

absorber elements (i.e., Cu, In, Ga, and Se) as expected. Na-related lines can also be observed for the as-received absorber, indicating Na-diffusion from the Mo-coated soda lime glass (SLG) back contact to the CIGSe surface due to the elevated sample temperature reached during absorber formation, a well-reported phenomenon.^[6] Furthermore, O and C-related XPS and Auger lines can be identified. While the signal of Na-related lines completely vanishes after the wet-chemical treatment steps, the O and C-related lines are mainly affected by the mild Ar⁺-ion treatment. As a result, the intensity of the O-related XPS and Auger lines is significantly reduced. A decrease in signal intensity to that extent cannot be observed for the C-related peaks, suggesting that, while the O is exclusively present at the CIGSe surface, C might (also) be incorporated into the CIGSe bulk.

Quantifying the XPS data (see Figure S2, Supporting Information), we find a Cu-poor (relative to the nominal 1:1:2 stoichiometry) absorber surface composition {i.e., [Cu] : ([In]+[Ga]) : [Se] = (1.0 ± 0.5) : (3.0 ± 0.6) : (6.0 ± 1.0)}, close to the 1:3:5 stoichiometry expected for absorbers fabricated by this particular production line^[7] and also reported for other high-efficiency CIGSe absorber surfaces.^[6,8] However, we note that besides being in agreement with the 1:3:5 phase formation, this result would not contradict the also suggested (Cu-free) reconstruction at chalcopyrite surfaces,^[8b] as the reason for the observed Cu-poor surface. To ultimately answer the question whether a 1:3:5 phase or a reconstructed (Cu-free) surface is responsible for the Cu-deficiency more experiments are needed. The effect of the surface Cu-depletion on the band gap of the CIGSe absorber near the surface will be discussed below.

Figure 1 shows the In 4d and Ga 3d core level spectra and respective peak fits of the data collected using different excitation energies. The spectra measured with 1253.56 eV (Mg K_α) and 1486.58 eV (Al K_α) excitations are significantly broader than the rest due to the broader excitation line widths of the non-monochromatized laboratory x-ray source compared to the synchrotron light sources (see Figure S3, Supporting Information). We find that the Ga

3d intensity decreases with increasing excitation energy (i.e., larger information depth, ID, for more details see Experimental Section and Figure S4, Supporting Information). However, this finding does not necessarily mean a Ga-enrichment towards the absorber surface. The In 4d and Ga 3d intensities in Figure 1 are greatly affected by changes in photoionization cross section (σ) in the employed excitation energy range (see Figure S5, Supporting Information). Photoionization of the Ga 3d electrons is favored over that of the In 4d electrons for lower excitation energies,^[9] as discussed below and in conjunction with **Figure 2a**.

Figure 2a shows the derived *intensity* ratios of the In 4d and Ga 3d core levels $\{I_{\text{Ga}}/[I_{\text{In}} + I_{\text{Ga}}]$, red hollow circles} as a function of the inelastic mean free path (IMFP) values of the probed photoelectrons, which follow the qualitative observation from Figure 1 that the Ga 3d intensity increases relative to the In 4d intensity with decreasing excitation energy and/or ID. [The signal detected for XPS core levels is effectively integrated over a volume defined by an exponential function that depends on the IMFP, which in turn increases with photoelectron kinetic energy (KE). Data measured with different excitation energies in this work are presented as a function of the IMFP to better illustrate from which sample region most (i.e., 63%) of the signal is derived. For more details on the relation between the IMFP of the measured photoelectrons and the ID of the measurements, see Experimental Section and Figure S4, Supporting Information.] Correcting the intensity ratio by the corresponding σ allows us to compute the $[Ga]/([In]+[Ga])$ ratio (black squares), which shows the opposite trend of $I_{\text{Ga}}/[I_{\text{In}} + I_{\text{Ga}}]$, i.e., not a Ga accumulation but a Ga depletion towards the CIGSe surface (see Ref. ^[10] for a critical assessment of this result). For measurements with IMFP values between 0.6 – 1.3 nm, we find a $[Ga]/([In]+[Ga])$ ratio that agrees (within the experimental uncertainty) well with the reported average bulk $[Ga]/([In]+[Ga])$ composition of 0.25 – 0.30 of absorbers from the same deposition batch,^[11] as probed by x-ray fluorescence analysis (XRF, displayed for comparison as the gray-shaded area in Figure 2a).

The ID of the XRF analysis is estimated to be several tens of μm , an order of magnitude higher than the thickness of the studied absorber layers,^[12] effectively providing an average composition value for the complete CIGSe thin-film, without resolving differences in $[\text{Ga}]/([\text{In}]+[\text{Ga}])$ gradients throughout the absorber profile designed to produce beneficial band gap gradings. For measurements with IMFP values between 2.3 – 8 nm, we find a significant deviation from the average bulk composition: a significant Ga accumulation in this region of the CIGSe. Because the $I_{(\text{Ga})}/[I_{(\text{In})} + I_{(\text{Ga})}]$ of the CIGSe absorber derived from the Advanced Light Source (ALS) measurements (i.e., 150 – 600 eV excitations) is consistent, irrespective of surface cleaning treatment (see Figure S6, Supporting Information), we believe that the lower Ga composition detected from measurements with IMFP values < 2 nm is not an effect of the KCN etch cleaning procedure. The identified Ga accumulation derived from measurements with IMFP values between 2.3 – 8 nm is consistent with the intentionally introduced compositional grading design of high-efficiency CIGSe absorbers,^[4,7] aiming for a higher Ga content at the front side and back side of the absorber to enhance current collection and minimize charge carrier recombination at the contacts. Front side $[\text{Ga}]/([\text{In}]+[\text{Ga}])$ grading profile trends have been observed for similar CIGSe absorbers in various sputter depth profile studies before.^[5a,7] However, the detected span of the grading depth in these studies (i.e., c. 500 nm) is two orders of magnitude greater than our presented results, where we can identify a pronounced step in Ga content for measurements with IMFP values > 2 nm. Sputtering-based depth profile techniques generally do not provide dependable composition information in this depth regime due to preferential sputtering processes inherent to these type of destructive analysis techniques, which is especially critical in the time prior to the onset of etching equilibrium conditions, i.e. at the start of the sputtering process which is related to the surface near sample region.

The lower Ga content derived from measurements with IMFP values < 2 nm could be interpreted as an In-accumulation in the topmost region of the absorber surface. Similar In-

rich surfaces are seen in small-area high-performing CIGSe absorbers prepared by other groups, which deliberately end their absorber growth process with an In-termination step.^[8a,13] Such finishing treatments are, however, very unlikely in the 30 cm × 30 cm in-line deposition machine used to prepare the studied samples, even if the evaporation sources would be adjusted to intentionally achieve such an In-terminated surface (i.e., in contrast to a static CIGSe deposition method). In the present case, the formation of a more In-rich (i.e., Ga-poor) surface could be explained by Cu-vacancy-mediated In and Ga diffusivity processes in chalcopyrite materials.^[14] Because it is more energetically-favorable for In to diffuse through Ga-rich CIGSe than for Ga to diffuse through In-rich CIGSe, we surmise that the faster In migration produces an In-rich (i.e., Ga-poor) absorber surface, while the slower diffusivity of Ga helps conserve the beneficial Ga gradings in the bulk of the absorber.^[14]

A common approach found in literature to assess the optical properties of chalcopyrite absorbers is to indirectly derive its band gap from its elemental composition. In an attempt to evaluate the efficacy of this practice, E_g values have been computed according to Equation (1),^[15] based on the determined $x = [\text{Ga}]/([\text{In}]+[\text{Ga}])$ ratios shown in Figure 2a, and are then compared to directly-measured E_g^{surf} values of absorbers with surface compositions similar to the investigated ZSW CIGSe absorber. (It is noted that, as in the case of the $x = [\text{Ga}]/([\text{In}]+[\text{Ga}])$ ratios, the resulting computed E_g values reflect the composition throughout the probing ID of the measurements using different excitation energies.)

$$E_g(x) = (1.00 + 0.13x^2 + 0.55x) \text{ eV} \quad (1)$$

The computed E_g values are shown in Figure 2b, which range from (1.2 ± 0.2) eV (for measurements with an IMFP value of 0.6 nm) to (1.3 ± 0.2) eV (for measurements with an IMFP value of 5 nm) and agree well (within the experimental uncertainty) with the E_g value computed for the XRF-derived bulk composition (gray-shaded area: 1.16 ± 0.02 eV) and the absorber E_g derived from quantum efficiency measurements (i.e., ~ 1.2 eV).^[7] However, as Equation (1) is only valid for chalcopyrite absorbers with an uniform Cu : In+Ga : Se

composition of 1:1:2 – which we have shown above is not the case for the absorber surface – the computed E_g values do not represent the real situation at the CIGSe surface.^[4b] In order to assess the effect of the strong surface Cu-deficiency of the absorber on its E_g^{surf} , we compare a range of E_g^{surf} values directly measured by combining UV (UPS) and inverse (IPES) photoemission spectroscopies, reported for CIGSe absorbers with surface compositions similar to the one of the analyzed sample.^[16] [In this case, the KE of photoelectrons derived from the valence band maximum (VBM) edge is ~ 40 eV; whereas, the electron KE range for IPES measurements at the conduction band minimum (CBM) edge is ~ 7 eV. Based on the “universal curve” of electron λ as a function of KE,^[17] the IMFP value for these techniques (combined) is estimated to range between 0.4 nm (for UPS) and 2 nm (for IPES), denoted by the width of the range of directly-measured E_g^{surf} values in Figure 2b.] We find that the E_g values computed from the derived $[\text{Ga}]/([\text{In}]+[\text{Ga}])$ ratio are significantly lower than the E_g^{surf} values determined by UPS and IPES (i.e., 1.4 – 1.62 eV),^[16] as anticipated.

The presence of a widened E_g^{surf} (relative to the bulk E_g , E_g^{bulk}) is expected to play a crucial role on the energy level alignment (and thus the energetic barrier for charge-carrier transport or recombination) at the buffer/absorber interface.^[18] The difference between the indirectly derived E_g values shown in Figure 2b and the E_g^{surf} range of the UPS/IPES measurements of (comparable) absorber samples is, hence, suggested to be due to the deviation of the surface composition of a *real-world* CIGSe thin-film solar cell absorber from common assumption with respect to stoichiometry (here the degree of Cu-deficiency at the CIGSe surface seems to be the crucial factor) and homogeneity. Based on these findings, we conclude that the E_g values computed from the $[\text{Ga}]/([\text{In}]+[\text{Ga}])$ of chalcopyrite absorbers with Cu-deficient surfaces only represent a low boundary for the real E_g^{surf} .

Recent significant performance improvements have been reported to result from post-deposition treatments (PDT)^[1] of (annealed) chalcopyrite absorbers with alkali metal salts (e.g., NaF, KF, RbF, and CsF or a combination of these) prior to buffer deposition. First

reports show that (NaF and KF) PDTs induce distinct Cu- and Ga-depletions^[1e,19] and pronounced E_g widening at the surface.^[20] Hence, the approach of using non-destructive, excitation-energy dependent XPS to study the chemical and electronic near-surface structure profiles might also lend itself to reveal the underlying beneficial mechanism of PDTs. In this sense, the here reported study can be considered as a preparatory “proof-of-concept” work for future characterization of near-surface composition and electronic structure – in particular when experimental setups become more easily available that allow to tune the excitation energy from soft to hard x-rays, as well as have the capability of directly probing the unoccupied states at a sample surface.

3. Conclusion

In summary, we have used non-destructive, excitation-energy dependent XPS measurements to reveal the near-surface $[Ga]/([In]+[Ga])$ elemental composition of a CIGSe absorber with pronounced Cu surface deficiency. We find the uppermost surface to be Ga-poor, which may be associated to differences in migration barriers for In and Ga in the chalcopyrite substrate.^[14] The observed composition variations at or close to the CIGSe surface surely affect the electronic structure of the absorber material and, therefore, the band offset to the subsequent buffer layer, which directly influences solar cell parameters – particularly the open-circuit voltage. The discrepancy between band gap values computed from the observed near-surface $[Ga]/([In]+[Ga])$ composition gradient of the CIGSe absorber – a common (although incomplete) analysis approach – with directly measured E_g^{surf} values from literature reinforces that the Cu-deficiency, rather than the $[Ga]/([In]+[Ga])$ composition, of the absorber surface is the critical determining factor of the band gap energy. Based on these findings, we conclude that high-performance CIGSe absorbers, which are generally Cu-deficient at the surface, feature a pronounced band gap profile there. A widened band gap

toward the surface increases the energetic barrier for high-rate charge carrier recombination across the (presumably) defect-rich emitter/absorber interface.

4. Experimental Section

CIGSe absorbers: CIGSe absorbers with a power conversion efficiency potential of up to 18% were prepared at the Zentrum für Sonnenenergie- und Wasserstoff-Forschung Baden-Württemberg (ZSW) using a high-efficiency, large area (i.e., 30 cm × 30 cm) in-line solar cell production line by multi-stage co-evaporation of Cu, In, Ga and Se on Mo-coated soda lime glass (SLG) back contacts.^[7] A 2- μ m thickness of the deposited CIGSe thin-film was achieved with a nominal $[\text{Ga}]/([\text{In}]+[\text{Ga}]) \approx 0.3$. However, CIGSe samples prepared in this solar cell production line are known to exhibit increased $[\text{Ga}]/([\text{In}]+[\text{Ga}])$ gradients toward the front and back sides of the absorber layer,^[7,14] designed to produce beneficial band gap gradings.^[4] Although no post-deposition treatment (PDT) was performed on the produced CIGSe absorbers, it is known that Na diffuses from the SLG into the absorber in this type of material system.^[6]

Surface characterization: Laboratory-based x-ray photoelectron spectroscopy (XPS) measurements were carried out employing a SPECS PHOIBOS 150MCD-9 electron analyzer using non-monochromatized Mg and Al K_{α} excitation energies. The elemental surface composition of the absorber was derived by evaluating the intensity of the Cu 2p_{3/2}, In 3d_{3/2}, Ga 2p_{3/2}, and Se 3d_{5/2} core level peaks, as determined by curve fit analysis of the spectra conducted with the Fityk software.^[21] Voigt profile functions, along with linear backgrounds, were used for these fits. Spin-orbit doublets were fitted with two Voigt functions with intensity ratios set to obey the $2j+1$ multiplicity rule. The intensities of the XPS core levels were corrected to account for differences in inelastic mean free path (IMFP),^[22] photoionization cross section (σ),^[9] and the transmission function of the electron analyzer (T).^[23] The energy scale for these measurements was calibrated in accordance to Ref. ^[24].

Further excitation-energy-dependent XPS measurements of the In 4d and Ga 3d core level region were conducted at Beamline 8.0.1^[25] of the Advanced Light Source (ALS) with soft x-rays and at the SPring-8 BL15XU beamline^[26] in the hard x-ray energy regime, allowing for an XPS characterization in an excitation energy range of 150 – 5950 eV. The endstations at the ALS and at SPring-8 are equipped with a SPECS PHOIBOS 150MCD-9 and a VG SCIENTA R4000 electron analyzer, respectively.^[25,26] Each of the measured In 4d and Ga 3d spectra was fitted following the approach described above. IMFP values in CIGSe for the selected excitation energies were calculated with the TPP-2 formula using the Quases-Tougaard computer code, yielding an effective, exponentially decreasing probing ID (taken as $3 \times \text{IMFP}$, a thickness from which 95% of the signal originates) range between 1.7 – 24.4 nm for the set of conducted experiments. However, results in this work are presented as a function of IMFP of the measurements to better highlight from which sample region most of the signal of the XPS measurements [i.e., $1 - (1/e) \sim 63\%$] is derived (see Figure S4, Supporting Information, for more details).^[22] To minimize the uncertainties related to the use of three different experimental setups, the quantification of the photoelectron spectroscopy data is limited to the In 4d and Ga 3d shallow core levels: Because of the energetic proximity of the In 4d and Ga 3d peaks, the impact of differences in IMFP and T on the spectral intensity for a given excitation energy is negligible. In this arrangement, the core level intensities need to be only normalized by their respective σ .^[9] Included in the used σ values is a correction for the angular distribution of the photoelectrons, which is dependent on the measurement geometry and the polarization of the x-rays. The energy scales of the synchrotron-based measurements were calibrated by measuring the Au 4f and the Fermi edge (E_F) of an Au reference sample.

Sample handling: Samples were shipped from ZSW after being sealed in an inert atmosphere in order to minimize exposure to air (less than 5 minutes). Upon arrival at Helmholtz-Zentrum Berlin für Materialien und Energie GmbH (HZB), they were stored in an ultra-high vacuum (UHV) chamber until their characterization. Similar sample packing precautions were

employed for the transport of samples outside the HZB for experimental campaigns. The surface of the investigated CIGSe absorber was cleaned inside a N₂-filled glovebox directly attached to the surface analysis system by a 1 min aqueous ammonia treatment (i.e., 1 M for 1 min at room temperature, followed by a thorough rinse in deionized water) and mild Ar⁺ ion treatments (ion energies up to 250 eV) for short time periods (of 30 min cycles) before laboratory-based XPS measurements. Corresponding XPS survey spectra documenting the cleaning effect of the individual treatment steps are shown in Supporting Information (see Figure S1, Supporting Information). An aqueous KCN etch treatment (i.e., 1.5 M for 3 min at room temperature, followed by a thorough rinse in deionized water – a procedure that has been shown to clean air-exposed CIGSe surfaces effectively without otherwise significantly changing surface composition)^[27] was employed to clean the surface of the CIGSe absorber investigated with soft x-rays at the ALS. The KCN etch treatment was conducted immediately after the sample was removed from its sealed package. To minimize sample exposure to air, the cleaned CIGSe sample was left in deionized water for approximately 15 minutes until it was mounted (during this process, a thin film of deionized water was left on the surface of the sample) and introduced into the loadlock of the ALS endstation. Note, however, that the as-received CIGSe absorber surface has also been characterized at the ALS for comparison. The CIGSe absorber probed at SPring-8 was not subjected to surface cleaning treatments because the used hard x-ray excitation results in measurements that are less influenced by surface contaminants^[28] (compared to the other soft x-ray-based XPS measurements).

Supporting Information

Supporting Information is available from the Wiley Online Library or from the author.

Acknowledgements

This work was supported in part by the Helmholtz-Association (VH-NG-423). The ALS is supported by the Department of Energy, Basic Energy Sciences, Contract No. DE-AC02-05CH11231. The XPS measurements at SPring-8 were performed under the approval of NIMS Synchrotron X-ray Station (Proposal Nos. 2011A4609 and 2012B4610). R.F. is also grateful to the German Academic Exchange Agency (DAAD; 331 4 04 002) for financial

support. One of the authors (S.U.) would like to thank HiSOR, Hiroshima University and JAEA/SPring-8 for the development of HAXPES at BL15XU of SPring-8.

Received: ((will be filled in by the editorial staff))

Revised: ((will be filled in by the editorial staff))

Published online: ((will be filled in by the editorial staff))

References

- [1] a) Press Release: Solar Frontier Achieves World Record Thin-Film Solar Cell Efficiency of 22.9%, Tokyo, December 20, 2017, http://www.solar-frontier.com/eng/news/2017/1220_press.html (accessed: October, 2018); b) P. Jackson, R. Wuerz, D. Hariskos, E. Lotter, W. Witte, M. Powalla, *Phys. Status Solidi RRL* **2016**, *10*, 583; c) P. Jackson, D. Hariskos, R. Wuerz, O. Kiowski, A. Bauer, T. M. Friedlmeier, M. Powalla, *Phys. Status Solidi RRL* **2015**, *9*, 28; d) P. Jackson, D. Hariskos, R. Wuerz, W. Wischmann, M. Powalla, *Phys. Status Solidi RRL* **2014**, *8*, 219; e) A. Chirilă, P. Reinhard, F. Pianezzi, P. Bloesch, A. R. Uhl, C. Fella, L. Kranz, D. Keller, C. Gretener, H. Hagendorfer, D. Jaeger, R. Erni, S. Nishiwaki, S. Buecheler, A. N. Tiwari, *Nat. Mater.* **2013**, *12*, 1107.
- [2] a) L. Stolt, presented at IWG-CIGSTech 5 Solibro CIGS to the next level, Berlin, Germany (April, **2014**); b) K. Kushia, presented at IWG-CIGSTech 5 Current Status and Future Prospects of Solar Frontier, Berlin, Germany (April, **2014**); c) P. Jackson, D. Hariskos, E. Lotter, S. Paetel, R. Wuerz, R. Menner, W. Wischmann, M. Powalla, *Prog. Photovoltaics: Res. Appl.* **2011**, *19*, 894.
- [3] a) Press release: Fraunhofer ISE Pushes World Record for Multicrystalline Silicon Solar Cells to 22.3 Percent, September 25, 2017, <https://www.ise.fraunhofer.de/en/press-media/press-releases/2017/fraunhofer-ise-pushes-world-record-for-multicrystalline-silicon-solar-cells-to-22-point-3-percent.html> (accessed: October, 2018).

- [4] a) A. Chirilă, S. Buecheler, F. Pianezzi, P. Bloesch, C. Gretener, A. R. Uhl, C. Fella, L. Kranz, J. Perrenoud, S. Seyrling, R. Verma, S. Nishiwaki, Y. E. Romanyuk, G. Bilger, A. N. Tiwari, *Nat. Mater. Sol. Cells* **2011**, *10*, 857; b) R. Félix, A. Weber, O. Zander, H. Rodriguez-Álvarez, B.-A. Schubert, J. Klaer, R. G. Wilks, H.-W. Schock, R. Mainz, M. Bär, *J. Mater. Chem. A* **2019**, *7*, 2087.
- [5] a) M. Powalla, P. Jackson, W. Witte, D. Hariskos, S. Paetel, C. Tschamber, W. Wischmann, *Sol. Energy Mater. Sol. Cells* **2013**, *119*, 51; b) A. Eicke, T. Ciba, D. Hariskos, R. Menner, C. Tschamber, W. Witte, *Surf. Interface Anal.* **2013**, *45*, 1811.
- [6] a) D. Schmid, M. Ruckh, F. Grunwald, H.-W. Schock, *J. Appl. Phys.* **1993**, *73*, 2902; b) D. Schmid, M. Ruckh, H.-W. Schock, *Sol. Energy Mater. Sol. Cells* **1996**, *41-42*, 281.
- [7] G. Voorwinden, R. Kniesen, P. Jackson, M. Powalla, in *Proceedings of the 22nd European Photovoltaic Solar Energy Conference* **2007**, 2115.
- [8] a) M. Bär, I. Repins, M. A. Contreras, L. Weinhardt, R. Noufi, C. Heske, *Appl. Phys. Lett.* **2009**, *95*, 052106; b) D. Liao, A. Rockett, *Appl. Phys. Lett.* **2003**, *82*, 2829.
- [9] a) M. B. Trzhaskovskaya, V. I. Nefedov, V. G. Yarzhemsky, *At. Data Nucl. Data Tables* **2001**, *77*, 97; b) M. B. Trzhaskovskaya, V. K. Nikulin, V. I. Nefedov, V. G. Yarzhemsky, *At. Data Nucl. Data Tables* **2006**, *92*, 245; c) G. Rossi, I. Lindau, L. Braicovich, I. Abbati, *Phys. Rev. B* **1983**, *28*, 3031; d) K. K. Chin, K. Miyano, R. Cao, T. Kendelewicz, J. Yeh, I. Lindau, W. E. Spicer, *J. Vac. Sci. Technol. B* **1987**, *5*, 1080.
- [10] Because the peak intensity – relative concentration trend inversion is caused by the correction of the Ga 3d and In 4d line intensities by the derived σ changes, this finding critically depends on the assumption that the values taken from Refs. ^[9a,9b] derived by

interpolation to the relevant photoelectron energies (specifically for the σ of the In 4d line using 150 eV excitation energy, see Figure S4a) and their correction for the different angular photoelectron distributions (for the three employed experimental setups) are correct. In order to further reduce this intricate experimental uncertainty, we acknowledge that an experiment, including the thorough characterization of suitable reference compounds of known composition in the near-surface region, should ideally be performed in a single experimental endstation that allows tuning the excitation energy in a similar range (i.e., 150 – 5950 eV). Until access to such an infrastructure [of which only one is currently operational worldwide: I09 setup at Diamond Light Source (<http://www.diamond.ac.uk/Beamlines/Surfaces-and-Interfaces/I09.html>); and another one is about to get online: EMIL located at BESSY II (https://www.helmholtz-berlin.de/projects/emil/index_en.html)] becomes (more) available, the here employed approach represents the current state of the art.

- [11] W. Witte, Personal Communication, 2014.
- [12] B. L. Henke, E. M. Gullikson, J. C. David, *At. Data Nucl. Data Tables* **1993**, *54*, 181.
- [13] I. Repins, M. A. Contreras, B. Egaas, C. DeHart, J. Scharf, C. L. Perkins, B. To, R. Noufi, *Prog. Photovolt.: Res. Appl.* **2008**, *16*, 235.
- [14] W. Witte, D. Abou-Ras, K. Albe, G. H. Bauer, F. Bertram, C. Boit, R. Brüggemann, J. Christen, J. Dietrich, A. Eicke, D. Hariskos, M. Maiberg, R. Mainz, M. Meessen, M. Müller, O. Neumann, T. Orgis, S. Paetel, J. Pohl, H. Rodriguez-Alvarez, R. Scheer, H.-W. Schock, T. Unold, A. Weber, M. Powalla, *Prog. Photovolt.: Res. Appl.* **2015**, *23*, 717.
- [15] M. Bär, W. Bohne, J. Röhrich, E. Strub, S. Lindner, M. C. Lux-Steiner, C.-H. Fischer, T. P. Niesen, F. Karg, *J. Appl. Phys.* **2004**, *96*, 3857.

- [16] a) M. Morkel, L. Weinhardt, B. Lohmüller, C. Heske, E. Umbach, W. Riedl, S. Zweigart, F. Karg, *Appl. Phys. Lett.* **2001**, *79*, 4482; b) D. Hauschild, D. Kreikemeyer-Lorenzo, P. Jackson, T. Magorian Friedlmeier, D. Hariskos, F. Reinert, M. Powalla, C. Heske, L. Weinhardt, *ACS Energy Lett.* **2017**, *2*, 2383; c) M. Bär, S. Nishimaki, L. Weinhardt, S. Pookpanratana, W. N. Shafarman, C. Heske, *Appl. Phys. Lett.* **2008**, *93*, 042110.
- [17] M. P. Seah, W. A. Dench, *Surf. Interface Anal.* **1979**, *1*, 2.
- [18] R. Scheer, *J. Appl. Phys.* **2009**, *105*, 104505.
- [19] a) E. Handick, P. Reinhard, R. G. Wilks, F. Pianezzi, T. Kunze, D. Kreikemeyer-Lorenzo, L. Weinhardt, M. Blum, W. Yang, M. Gorgoi, E. Ikenaga, D. Gerlach, S. Ueda, Y. Yamashita, T. Chikyow, C. Heske, S. Buecheler, A. N. Tiwari, M. Bär, *ACS Appl. Mater. Interfaces* **2017**, *9*, 3581; b) E. Handick, P. Reinhard, R. G. Wilks, F. Pianezzi, R. Félix, M. Gorgoi, T. Kunze, S. Buecheler, A. N. Tiwari, M. Bär, in 2016 IEEE 43rd Photovoltaic Specialists Conference (PVSC), Portland, OR, 0017-0021, **2016**.
- [20] E. Handick, P. Reinhard, J.-H. Alsmeier, L. Köhler, F. Pianezzi, S. Krause, M. Gorgoi, E. Ikenaga, N. Koch, R. G. Wilks, S. Buecheler, A. N. Tiwari, M. Bär, *ACS Appl. Mater. Interfaces* **2015**, *7*, 27414.
- [21] M. Wojdyr, *J. Appl. Crystallogr.* **2010**, *43*, 1126.
- [22] a) S. Tougaard, *QUASES-IMFP-TPP2M*, **2002**; b) S. Tanuma, C. J. Powell, D. R. Penn, *Surf. Interface Anal.* **1994**, *21*, 165.
- [23] M. P. Seah, G. C. Smith, *Surf. Interface Anal.* **1990**, *15*, 751.

- [24] D. Briggs, M. P. Frye (Eds.), in *Practical Surface Analysis: Auger and X-ray Photoelectron Spectroscopy*, Wiley, New York **1983**.
- [25] M. Blum, L. Weinhardt, O. Fuchs, M. Bär, Y. Zhang, M. Weigand, S. Krause, S. Pookpanratana, T. Hofmann, W. Yang, J. D. Denlinger, E. Umbach, C. Heske, *Rev. Sci. Instrum.* **2009**, *80*, 123102.
- [26] S. Ueda, Y. Katsuya, M. Tanaka, H. Yoshikawa, Y. Yamashita, S. Ishimaru, Y. Matsushita, K. Kobayashi, in *AIP Conference Proceedings*, Vol. 1234, AIP Publishing, Melville, NY, USA **2010**, 403.
- [27] J. Lehmann, S. Lehmann, I. Laueremann, T. Rissom, C. A. Kaufmann, M.-C. Lux-Steiner, M. Bär, S. Sadewasser, *J. Appl. Phys.* **2014**, *116*, 233502.
- [28] D. Gerlach, D. Wippler, R. G. Wilks, M. Wimmer, M. Lozac'h, R. Félix, S. Ueda, H. Yoshikawa, K. Lips, B. Rech, M. Sumiya, K. Kobayashi, M. Gorgoi, J. Hüpkes, M. Bär, *IEEE J. Photovolt.* **2013**, *3*, 483.

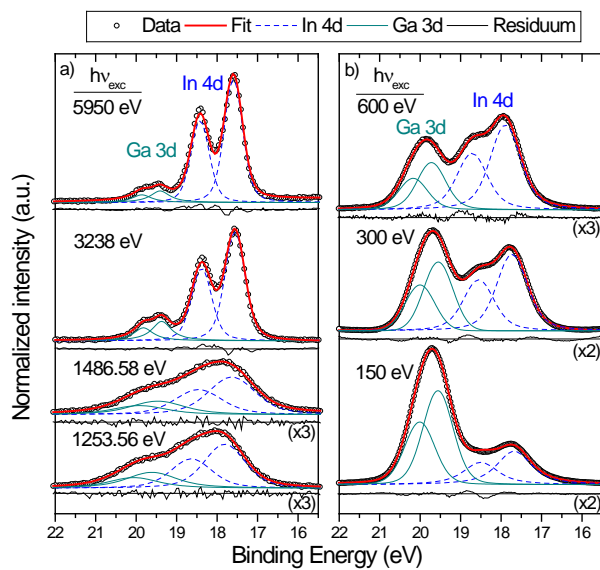


Figure 1. (a) and (b) XPS detail spectra of the In 4d and Ga 3d core level region of the CIGSe sample, including fits and respective residua, as measured with various excitation energies. Vertical offsets are added for clarity.

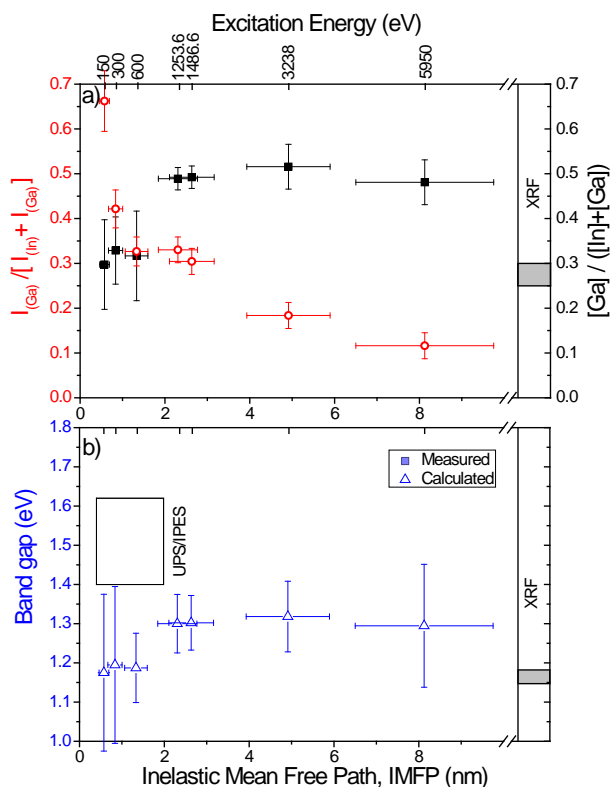


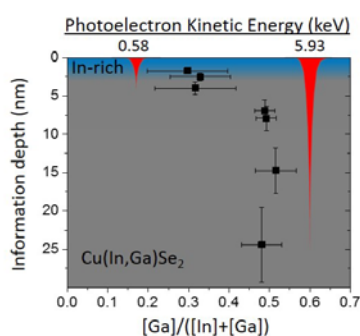
Figure 2. (a) Ratio of the Ga 3d (I_{Ga}) and In 4d (I_{In}) XPS core level intensities (red open circles, right axis) and of the derived $[\text{Ga}]/([\text{In}]+[\text{Ga}])$ composition (black squares, left axis) as a function of inelastic mean free path (IMFP) values of the excitation-energy-dependent measurements. The reported mean XRF-probed bulk $[\text{Ga}]/([\text{In}]+[\text{Ga}])$ composition of absorbers from the same deposition batch is also displayed as the gray-shaded area in the right extremity.^[11] (b) $E_{\text{g}}^{\text{bulk}}$ values computed for the $[\text{Ga}]/([\text{In}]+[\text{Ga}])$ ratios in (a) using Equation (1). For comparison, a range of directly-measured $E_{\text{g}}^{\text{surf}}$ values of absorbers with surface compositions similar to the one of the studied ZSW CIGSe absorber, from Ref. ^[16], is shown.

The chemical and electronic structure of industry-relevant Cu(In,Ga)Se₂ thin-film photovoltaic absorbers is presented. Compared to the bulk, a pronounced Cu-depletion is detected at the surface, as well as a Ga-poor (In-rich) composition in the topmost region of the material. Of these composition changes, the surface Cu-deficiency affects the electronic properties of the absorber most strongly.

Chalcopyrite Absorber Stoichiometry

Roberto Félix,* Wolfram Witte, Dimitrios Hariskos, Stefan Paetel, Michael Powalla, Mickael Lozac'h, Shigenori Ueda, Masatomo Sumiya, Hideki Yoshikawa, Keisuke Kobayashi, Wanli Yang, Regan G. Wilks, and Marcus Bär

Near-Surface [Ga]/([In]+[Ga]) Composition in Cu(In,Ga)Se₂ Thin-Film Solar Cell Absorbers – An Overlooked Material Feature



ToC figure